Peer-reviewed version available at *Molecules* **2017**, *22*, 2153; doi:10.3390/molecules22122153

*Article*

# Frozen Microemulsions for MAPLE Immobilization of Lipase

**Valeria Califano[1], Francesco Bloisi[2,*], Giuseppe Perretta[1], Antonio Aronne[3], Giovanni Ausanio[2], Aniello Costantini[3] and Luciano Vicari[2]**

[1] Istituto Motori-CNR, via G. Marconi 8, Napoli 80125, Italy. v.califano@im.cnr.it
[2] CNR-SPIN and Department of Physics, Università degli Studi di Napoli Federico II, Piazzale V. Tecchio 80, Napoli 80125, Italy ; bloisi@unina.it
[3] Department of Chemical Engineering, Materials and Industrial Production, Università degli Studi di Napoli Federico II, Piazzale V. Tecchio 80, Napoli 80125, Italy, anicosta@unina.it
* Correspondence: bloisi@unina.it; Tel.: +39-081-768-2585

**Abstract:** MAPLE (matrix assisted pulsed laser evaporation) depositions of Candida Rugosa lipase were carried out from ice matrices whose composition is optimized in order to minimize conformational damage of the protein, which strongly influences its catalytic activity. To induce lid opening and to protect lipase during the MAPLE process, pentane and m-DOPA amino acid were added to the liquid matrix giving a target formed by a frozen water-lipase-pentane microemulsion. FTIR and AFM were used to investigate the structure of MAPLE deposited lipase films. The ability of MAPLE films to promote transesterification was determined by thin layer chromatography. It was shown that m-DOPA has influence on the aggregation but not on the unfolding of lipase induced by MAPLE, while the microemulsion formed by the addition of pentane to the target composition is effective in protecting lipase during the MAPLE process. MAPLE deposited lipases showed a modified specificity.

**Keywords:** MAPLE; microemulsion; lipase; thin film..

## 1. Introduction

Lipases (E.C.3.1.1.3) are ubiquitous enzymes able to catalyze reactions of large industrial interest, such as hydrolysis, esterification and transesterification of long-chain acylglycerides. In particular, the enzymatic transesterification of vegetable oil into biodiesel allows treating raw materials with high content of free fatty acids (i.e. waste fried oil), enabling the use of low quality, reused and inedible oils without a negative impact on the environment. The widespread application of lipase in industry, however, is inhibited because milder, eco-friendly, highly selective enzymatic catalysis is not competitive with chemical catalysis due to the high cost of enzymes. Immobilizing enzymes on insoluble supports can address this issue by allowing re-use of the enzyme and continuous processing [1].

Matrix assisted pulsed laser evaporation (MAPLE) is a pulsed laser technique for thin film deposition, in which the target is composed of a frozen solvent (the matrix) containing a low volume fraction of the material to be deposited (the guest material). The matrix is a volatile, light absorbing solvent. When a laser beam impacts the target, droplets of both the volatile solvent and the solute are ejected away from the target. A vacuum system pumps away the matrix molecules, while the guest material deposits onto the substrate. The matrix absorbs most of the laser radiation giving a softer ejection mechanism with respect to pulsed laser deposition (PLD), hence transferring delicate molecules from the target to the substrate in undamaged form [2, 3]. Due to such attributes, MAPLE technique has been successfully used to deposit several proteins in an undamaged and functional form [4-8]. However, the MAPLE deposition of lipase is a sensitive issue, since lipases are unique enzymes in that they require interfacial activation for full catalytic performance. Actually, since lipids are water insoluble, lipases act on emulsified systems. Upon adsorption at a hydrophobic/hydrophilic interface, lipase undergoes a conformational change from the inactive to

the active conformation. This change is promoted by the movement of a helical loop from the 'closed' form in which the catalytic site is inaccessible to the 'open' active one. During the immobilization procedure the mechanism of interfacial activation must be preserved and lipase is preferably to be obtained in the 'open-lid' conformation, known to be more active [9].

Solvent assisted techniques for lipase immobilization affect its conformation by both the nature of the substrate and the adsorption conditions (i.e., pH of the solution). Benefits of using MAPLE for lipase immobilization include independence of lipase conformation on enzyme/support interaction, dry deposition allowing the use water-incompatible supports and the possibility of tailoring lipase conformation in solution. Lipase films were already obtained by MAPLE using a water matrix [10], but conformational analysis of the obtained films pointed out an important protein unfolding and aggregation/self-association. In this work, the matrix composition is improved by adding m-DOPA and pentane to the water matrix to obtain lipase films in which the secondary structure of the enzyme is preserved.

M-DOPA (3-(3,4-dihydroxyphenyl)-2-methyl-L-alanine) is an analogous of L-DOPA (3,4-dihydroxy-phenyl-L-alanine) with a methyl group added. L-DOPA is an unusual amino-acid residue found in the adhesive protein secreted by mussels and responsible for mussel fouling on a variety of surfaces. The catechol side chain of L-DOPA is thought to be responsible for the adhesive role of these proteins. The use of MAPLE for the deposition of m-DOPA was already discussed for improving PEG adhesion in anti-biofouling applications [11].

In this work, m-DOPA is added to reduce the risk of photochemical damages acting as a laser radiation absorber and to protect lipase against unfolding/aggregation that can occur during drying in plume expansion [12], whereas pentane is added to induce lid opening.

## 2. Results and discussion

The MAPLE deposition parameters are reported in table 1.

The choice of the laser wavelength has been set by the need of inducing as little damage as possible to the protein, since lipase has a large absorption band, centred at 280 nm [13], in the UV region normally used for MAPLE deposition and a N-H stretching vibration absorption in the IR region used for RIR-MAPLE (2900 nm) [14]. Our focus is the deposition of lipase with preserved tertiary structure, since in catalytic applications obtaining a smooth deposition is not essential. This suggested us to select a small substrate to target distance in order to maximize the deposition yield.

**Table 1.** MAPLE deposition parameters.

| | |
|---|---|
| Laser wavelength | 1064 nm |
| Laser pulse energy | 526-410 mJ/pulse |
| Pulse duration | 7 ns |
| Pulse repetition rate | 4 Hz |
| Number of pulses | 23000 |
| Target-substrate distance | 9 mm |
| Incidence angle | 45° |
| Chamber pressure during deposition | $10^{-4}$ Pa |
| Target temperature | -123°C |
| Substrate temperature | 25°C |
| Target matrix | distilled water |

Samples are obtained by varying the composition of the target solution, adding the excipient m-DOPA and the apolar solvent pentane to the lipase/water matrix system. The target composition and laser pulse energy used for each deposition are reported in table 2. The pulse energy used corresponds to the minimum value allowing target evaporation. One of these samples, M-CRL1, was already characterized in a previous work [10].

**Table 2.** Target composition of MAPLE deposited samples.

| Sample | Target composition | | | Pulse energy (mJ/pulse) |
|---|---|---|---|---|
| | Lipase | m-DOPA | Pentane | |
| M-CRL1 | 0.2% wt | - | - | 526 |
| M-CRL2 | 0.18% wt | 0.02% wt | - | 410 |
| M-CRL3 | 0.18% wt | 0.02% wt | 0.5% V/V | 410 |

M-DOPA was added because it absorbs the IR laser radiation, since the third overtone of C-H stretching of aromatic groups is located around 1064 nm [15], while water does not have absorption bands near that wavelength. Actually, m-DOPA lowers the ablation threshold of the target thus allowing using lower laser pulse energy, as indicated in table 2. Furthermore, m-DOPA acts as an excipient to protect lipase from denaturation induced during plume expansion by drying [12]. Pentane is added to induce lid opening and is responsible for the microemulsion formation. The addition of pentane, 0.5% in volume respect to the water, did not cause any phase separation or opalescence. Since pentane is poorly soluble in water (solubility at 25°C in molar fraction $x=1.2*10^{-5}$ [16] vs. $x=7.8*10^{-4}$ used in this work), we assume that a microemulsion was formed due to the amphiphilic nature of lipase [17]. A microemulsion is a spontaneously forming system comprising mixture of water, hydrocarbons and amphiphilic compounds forming thermodynamically stable, homogeneous (heterogeneous in molecular scale), optically isotropic solutions with particle sizes ranging from 5 to 100 nm [18]. MAPLE deposition from a frozen microemulsion target is feasible since protein stabilized emulsion, unlike other emulsified systems, have reduced tendency to phase separation during freezing [19, 20].

Infrared spectroscopy is a well-established technique for the conformational analysis of proteins [21] and has been used to study the secondary structure of proteins both in water solution [22, 23] and in the solid state [24, 25]. FTIR spectra of the three MAPLE-deposited samples, together with those of free-CRL are reported in figures 1 (a) (1300-1800 $cm^{-1}$ range) and 1 (b) (2600-4000 $cm^{-1}$ range), since the absorption of the various secondary structural elements of the protein backbone can be studied in these spectral regions. The spectra are normalized for the height of the band at 1655 $cm^{-1}$. In figure 1, the FTIR spectrum of free-CRL (trace d) shows four main absorption bands ascribed to the vibration modes of the protein backbone. The band in the 1600-1700 $cm^{-1}$ region, the amide I absorption band, centred at 1655 $cm^{-1}$, originates mainly from the C=O stretching vibration of the peptide group, whose frequency depends on the strength of hydrogen-bonds C=O---H-N and on the dipole-dipole interactions between carboxyl groups along the peptide chain. In turn, this is determined by the secondary structure adopted by the polypeptide chain and this band is therefore sensitive to the protein conformation [22]. This band consists of overlapping components representing secondary structure elements such as $\alpha$-helices, β-sheets, β-turns and disordered structures. Several methods have been developed to estimate quantitatively the relative contributions of different types of secondary structures. Among these, second derivative spectra allow the identification of various secondary structures present in the protein. Curve fitting procedure can then be applied to calculate quantitatively the area of each component representing a type of secondary structure. The band centred at 1540 $cm^{-1}$, amide II, is mainly related to the out-of-phase combination of the N-H in-plane bending and the C-N stretching vibration. This band also strongly depends on the secondary structure elements from which it originates, but the correlation structure/frequency is less straightforward. The amide III (1370-1480 $cm^{-1}$) derives mainly from the in phase combination of the N-H bending and the C-N stretching vibration; due to the complexity of these contributes there is not a direct correlation between the position of this band and the protein structure. The band at 3350 $cm^{-1}$, the amide A absorption band, is due to the stretching of the N-H bond. The frequency of the amide A vibration depends on the strength of the hydrogen

bond. In particular, N-H bonds in $\alpha$-helices and $\beta$-sheets absorb around 3300 $cm^{-1}$, while in random-coil structure the absorption band shifts to 3400 cm-1 [26].

By comparing the spectra of free-CRL and MAPLE deposited lipases (figure 2), three main differences are seen: in the spectra of MAPLE deposited lipases (i) the amide I band shifts towards lower wave-numbers; on the contrary, (ii) the amide A band shifts to higher wave-numbers. Moreover, (iii) the relative intensity of the amide II band is strongly reduced resulting partially overlapped with the amide I band for the M-CRL2 and M-CRL3. Further differences are seen in the 1300-1500 $cm^{-1}$ region: in the spectra of M-CRL1 and M-CRL2 a strong band centred at 1460 $cm^{-1}$ occurs whereas in the spectrum of M-CRL3 a weaker and smoother band is seen which resembles the envelope of the two bands occurring for the free-CRL.

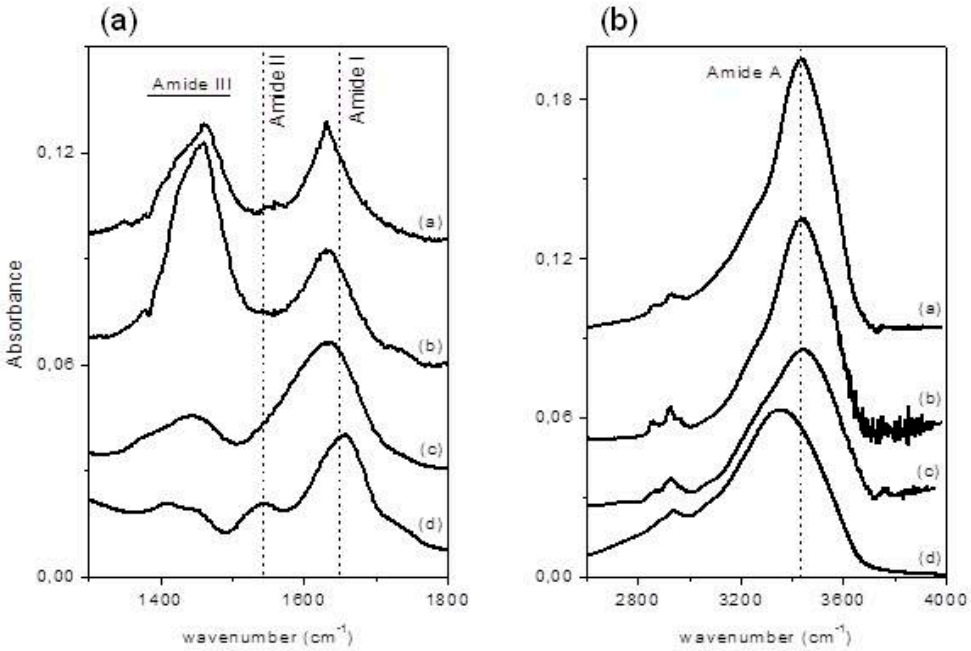


**Figure 1.** FTIR spectra of (a) M-CRL1 (b) M-CRL2 (c) M-CRL3 and (d) free-CRL. The spectra were normalized to the height of amide I absorption band.

The displacement of the amide I band towards lower wave-numbers was already attributed to an important phenomenon of protein unfolding/aggregation [10]. From the spectra of figure 1 it can be seen that this shift is more pronounced in M-CRL1 and M-CRL2 (about 27 $cm^{-1}$) than in M-CRL3 (about 20 $cm^{-1}$). To determine the degree of unfolding, a curve fitting procedure was applied to the spectra of the three MAPLE deposited spectra and compared with that of free lipase. The results are reported in table 3 while in figure 2 are illustrated the best fit Gaussian components obtained for M-CRL2 (trace (b)) and M-CRL3 (trace (a)). Since in these spectra the amide I and amide II bands are partially overlapped in the fitting procedure the amide II is considered as a component of the amide I band. Moreover, in the spectrum of M-CRL2 the amide III band is partially overlapped with the amide II one consequently, to avoid errors in the baseline correction, these two bands were included in the fitting procedure.

Preprints (www.preprints.org) | NOT PEER-REVIEWED | Posted: 21 September 2017 doi:10.20944/preprints201709.0105.v1

Peer-reviewed version available at Molecules 2017, 22, 2153; doi:10.3390/molecules22122153



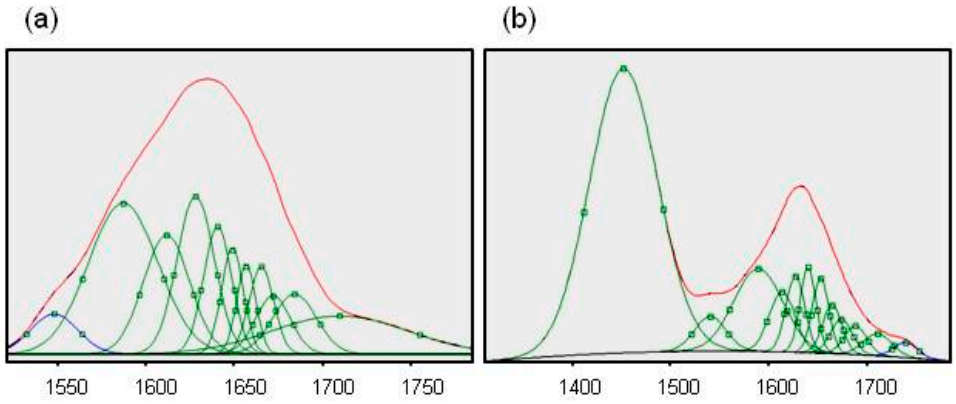


**Figure 2.** Best fit Gaussian components of amide I of (a) M-CRL3 and (b) M-CRL2.

**Table 3.** Component band position($cm^{-1}$) and assignment of the best-fit Gaussian components of the amide I band.

| Gaussian component position ($cm^{-1}$) | | | | Attribution | Literature data |
|---|---|---|---|---|---|
| Free CRL | M-CRL1 | M-CRL2 | M-CRL3 | | |
| | 1566 | 1539 | 1548 | Amide II | 1530-1550 [25] |
| | 1585 | 1588 | 1587 | C=O stretching of $COO^-$ | 1565-1585 [25] |
| 1609 | 1618 | 1613 | 1612 | Intermolecular H-bonded C=O (aggregates) | 1610-1620 [24] |
| 1623 | | 1626 | 1629 | β-sheets | 1620-1650 [24] |
| 1635 | 1631 | | | | |
| 1640 | 1642 | 1639 | 1641 | Disordered structures | 1640-1650 [27] |
| 1650 | 1650 | 1652 | 1650 | α-helices | 1650-1660 [24] |
| 1659 | 1657 | | 1658 | | |
| 1668 | 1667 | 1663 | 1666 | β-turns | 1660–1690 [24] |
| 1676 | | 1673 | 1673 | | |
| 1685 | 1696 | 1687 | 1685 | ⌾-turns/⌾-sheets | 1680-1696 [27, 28] |
| 1711 | 1738 | 1710 | 1711 | C=O stretching of -COOH | |

The Gaussian components at wavenumbers smaller than 1590 $cm^{-1}$ are attributable to components of amide II band overlapping with amide I, while the component occurring in the 1580-1590 $cm^{-1}$ range is due to the C=O stretching of the COO- aspartic and glutamic acid side chain.

Peer-reviewed version available at Molecules 2017, 22, 2153; doi:10.3390/molecules22122153



As matter of the fact, based on the values of lipase pKa, Asp and Glu side chains are largely deprotonated at the matrix pH. The components at wavenumbers higher than 1610 $cm^{-1}$ are related to the C=O stretching in the various conformational environment of the protein (α-helices, β-sheets, β-turns and disordered structures, intermolecular β-strands). From the area of each of these components, it is possible to evaluate the percentage of the secondary structure elements for the four samples. The results are reported in table 4.

**Table 4.** Percentage of the secondary structure elements.

| Structural element | Free-lipase | M-CRL1 | M-CRL2 | M-CRL3 |
|---|---|---|---|---|
| β-sheets | 25.4 | 14.5 | 18.1 | 23.4 |
| α-helices | 27.2 | 21.3 | 15.6 | 15.4 |
| β-turns | 16.3 | 14.7 | 21.3 | 16.1 |
| β-turns/ β-sheets | 13.7 | 4.3 | 8.1 | 10.1 |
| Aggregates | 14.8 | 27.8 | 19.6 | 21.1 |
| Disordered | 2.6 | 17.4 | 17.3 | 13.9 |

CRL conformation was determined by X-ray diffraction on lipase crystals [29, 30]. XRD data revealed in the CRL open conformation a content 30% for α-helices and 12% for β-sheets. In this study, the content of α -helices of free lipase is lower and that of β-sheets higher with respect to X-ray diffraction data. This is ascribable to the process of lyophilisation. Proteins composed of α-helices and mixtures of α-helices and β-sheets have generally shown reversible conformational changes upon freeze-drying. Most commonly, a significant decrease in α-helix content is detected, with a simultaneous increase in β-sheet formation (possibly intramolecular in nature), as occurs in the free lipase sample under study. Furthermore, the presence of intermolecular β-sheets due to aggregation is detected (14.8% aggregates in free CRL). MAPLE deposited samples show a decrease in the β-sheet content which is dramatic in M-CRL1 sample and attenuates going towards the M-CLR3 sample. Contextually, the content of α-helices falls. In M-CRL1 sample the content of intramolecular aggregates is 27.8%, but it falls at 19.6% in M-CRL2 sample, indicating that the addition of m-DOPA is effective in reducing the phenomenon of lipase self-association, likely by providing hydrogen bonds during the freezing of the MAPLE target and drying in plume expansion. Nevertheless, there is still a certain degree of unfolding, as testified by the high percentage of disordered structures, comparable with those of M-CRL1 sample. The degree of unfolding decreases in the M-CRL3 sample, confirming that the formation of a microemulsion target is efficient in better preserving the polypeptide conformation during the MAPLE process.

This interpretation can be substantiated by the analysis of amide A band in the 3000-3700 $cm^{-1}$ region. Curve fitting of the amide A band for the three MAPLE-deposited lipases was performed giving two Gaussian components for all samples (see table 5). In this region the contribute related to the O-H stretching of water can be considered to have a little influence in the overall absorption, since it was demonstrated that the MAPLE process is effective in removing water from the deposited samples [31]. Therefore, the peaks at about 3300 $cm^{-1}$ and 3420 $cm^{-1}$ can be related to hydrogen-bonded N-H stretching vibrations and to vibrations of free N-H groups of the unfolded peptide forms [32], respectively.

**Table 5.** Results of amide A Gaussian deconvolution: Gaussian peak positions (cm-1), peak area, A, percentage peak area, A%, and the relative unfolding evaluated as percentage ratio of the area of M-CRL2 and M-CRL3 peak 2 with respect to that of M-CRL1.

| Sample | Peak 1<br>Peak 2<br>position ($cm^{-1}$) | Peak area<br>A | A% | Relative unfolding<br>% |
|---|---|---|---|---|
| M-CRL1 | 3222.5±4.8<br>3451.5±1.2 | 5.9±0.29<br>24.0±0.29 | 19.7 | 100 |
| M-CRL2 | 3251.2±6.8<br>3455.2±1.8 | 4.9±0.37<br>19.8±0.37 | 80.3 | 99.9 |
| M-CRL3 | 3322.7±8.1<br>3494.8±3.3 | 9.76±0.68<br>9.97±0.67 | 19.8 | 62.9 |

Since N-H and N-H--O bonds have different dipole moments, resulting in different intensities of the respective absorption bands, the percentage area of the peak 2 is not directly correlated with the degree of unfolding of the protein, even if its value decreases going from M-CRL1 to M-CRL3. To give a relative measure of the percentage of unfolding occurring in M-CRL2 and M-CRL3 with respect to M-CRL1, that can be considered the more unfolded sample, the percentage ratio of the area of M-CRL2 and M-CRL3 peak 2 with respect to that of M-CRL1 was considered (see Table 3). The percentage of reduction of unfolding in M-CRL2, equal to 0.1%, is very small, while it becomes relevant in M-CRL3, resulting in a reduction of unfolding of 37.1%.

In figure 3 optical micrographs of M-CRL2 and M-CRL3 are shown. As displayed in figure 3 (a), M-CRL2 film is formed by micrometric clusters and crystalline inclusions, some of which are evidenced by white circles. These features outline that m-DOPA is effective in absorbing the infrared laser radiation thanks to its catechol side chain, its addition to the matrix target causing the deposition of a larger mass of material at a lower laser pulse energy with respect to the sole lipase/ice target [10]. The formation of micrometric clusters evidenced in Fig. 3 has often been observed in MAPLE deposition [33-35, 11]. It depends on the explosive disintegration of the target hit by the laser that gives rise to the ejection of a mixture of vapor-phase molecules, small molecular clusters and droplets [36]. The solvent begins to evaporate during the flight from the target, so that the solute concentration in droplets and clusters increases causing the deposition of micrometric aggregates. The surface of M-CRL3 film, on the contrary, is much smoother with no visible clusters at the optical microscope, figure 3(b), indicating a better molecular dispersion of lipase, possibly due to its adsorption at the pentane nano-droplets of the microemulsion target.

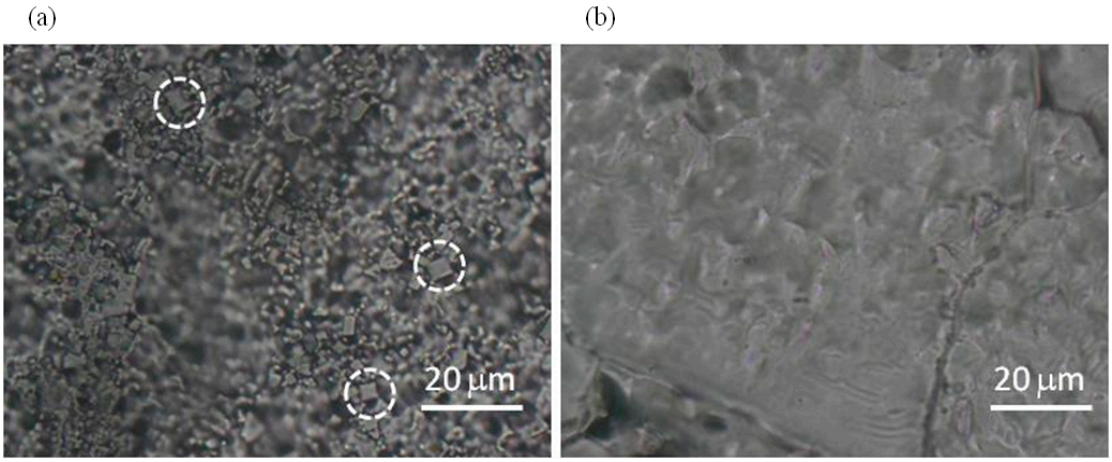


**Figure 3.** micrographs of (a) M-CRL2 and (b) M-CRL3. White circles highlight crystalline inclusions.

Peer-reviewed version available at Molecules 2017, 22, 2153; doi:10.3390/molecules22122153



To further investigate the morphology of M-CRL3, AFM images of the sample were acquired in different region of the samples. Some of such images are compared with the ones of M-CRL1 film [10] in figure 4. Particularly, 4 μm x 4 μm (left) and 1 μm x 1 μm (right) AFM images of M-CRL1 film are displayed in figure 4 (a), while 4 μm x 4 μm (left) and 1 μm x 1 μm (right) AFM image of M-CRL3 film are shown in figure 4 (b). From AFM images of M-CRL1 it is evident that the substrate was uniformly covered by nanometric aggregates that are due to lipase self-association. These aggregates have mean planar dimension of 40 nm. Considering that lipase is a globular protein of approximately 5 nm in diameter, aggregates are composed of several lipase globules.

Figure 4(b) shows a different morphology for M-CRL3 film. As seen in the lower magnification picture, clusters are much smaller and concentrated in droplet-like regions of about ≤ 1 μm in size, while at the nanometric level the compact structure of aggregates of 40 nm is not present, instead much smaller features are detected from the higher magnification picture, confirming a reduction of self-association of proteins as already suggested by FTIR analysis.

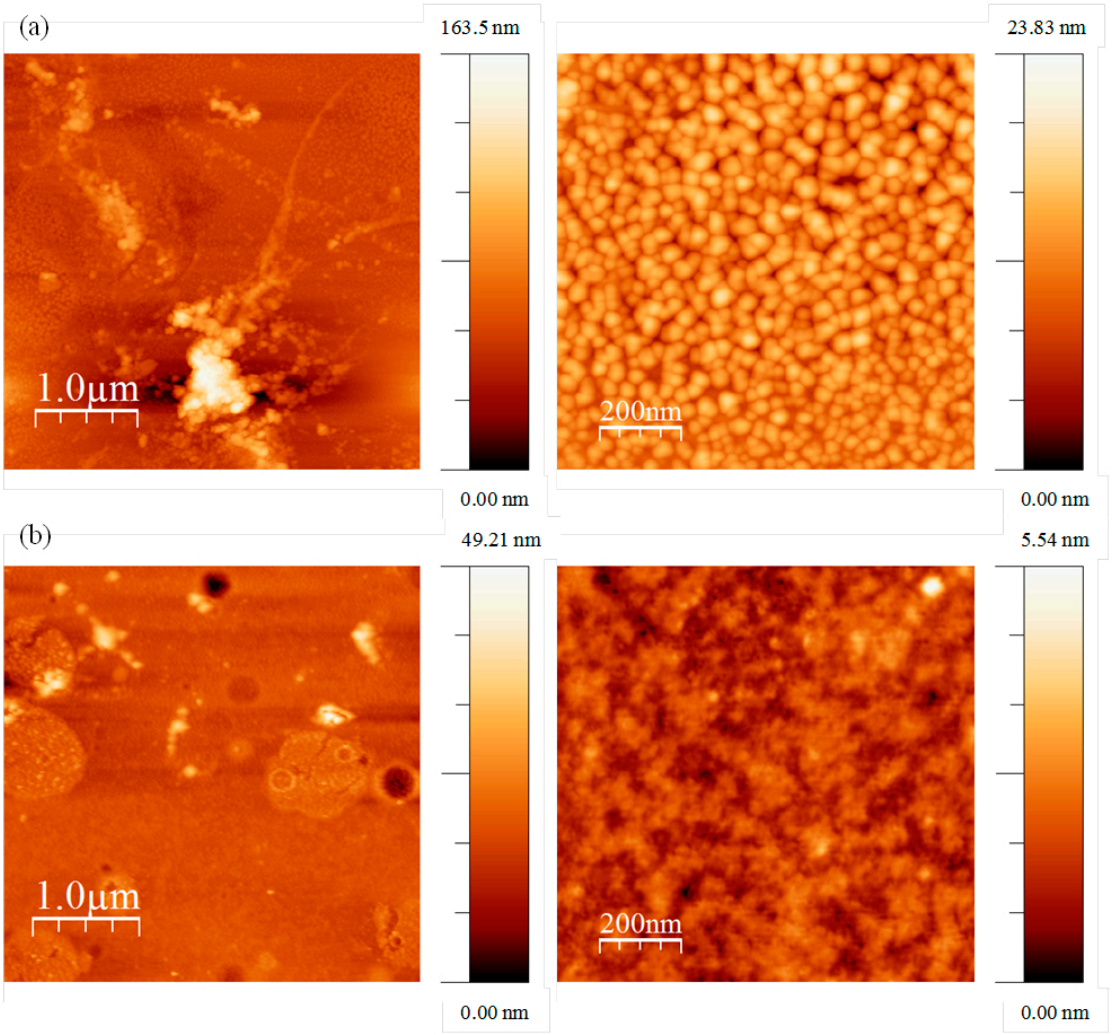


**Figure 4.** a) 4 μm x 4 μm (left) and 1 μm x 1 μm (right) AFM images of M-CRL3 film; (b): 4 μm x 4 μm (left) and 1 μm x 1 μm (right) AFM image of M-CRL1 film.

Preliminary tests of the deposited lipase samples were performed by transesterification reaction carried out between soybean oil and isopropyl alcohol using RP-TLC to identify the reaction products. In figure 5 the chromatograms of the three samples (M-CRL1 in fig.5c, M-CRL2 in fig.5d and M-CRL3 in fig.5e) are compared with that obtained using 1mg (fig.5b) of free CRL as catalyst. The amount of 1 mg was chosen since this is the order of magnitude of the amount of lipase

Preprints (www.preprints.org) | NOT PEER-REVIEWED | Posted: 21 September 2017 doi:10.20944/preprints201709.0105.v1

Peer-reviewed version available at Molecules 2017, 22, 2153; doi:10.3390/molecules22122153



deposited by MAPLE. For sake of clarity the chromatogram of unreacted oil (fig.5a) and that obtained using 15 mg of free CRL as catalyst (fig.5f) are also reported. The amount of 15mg has been chosen to clearly show the action of lipase.

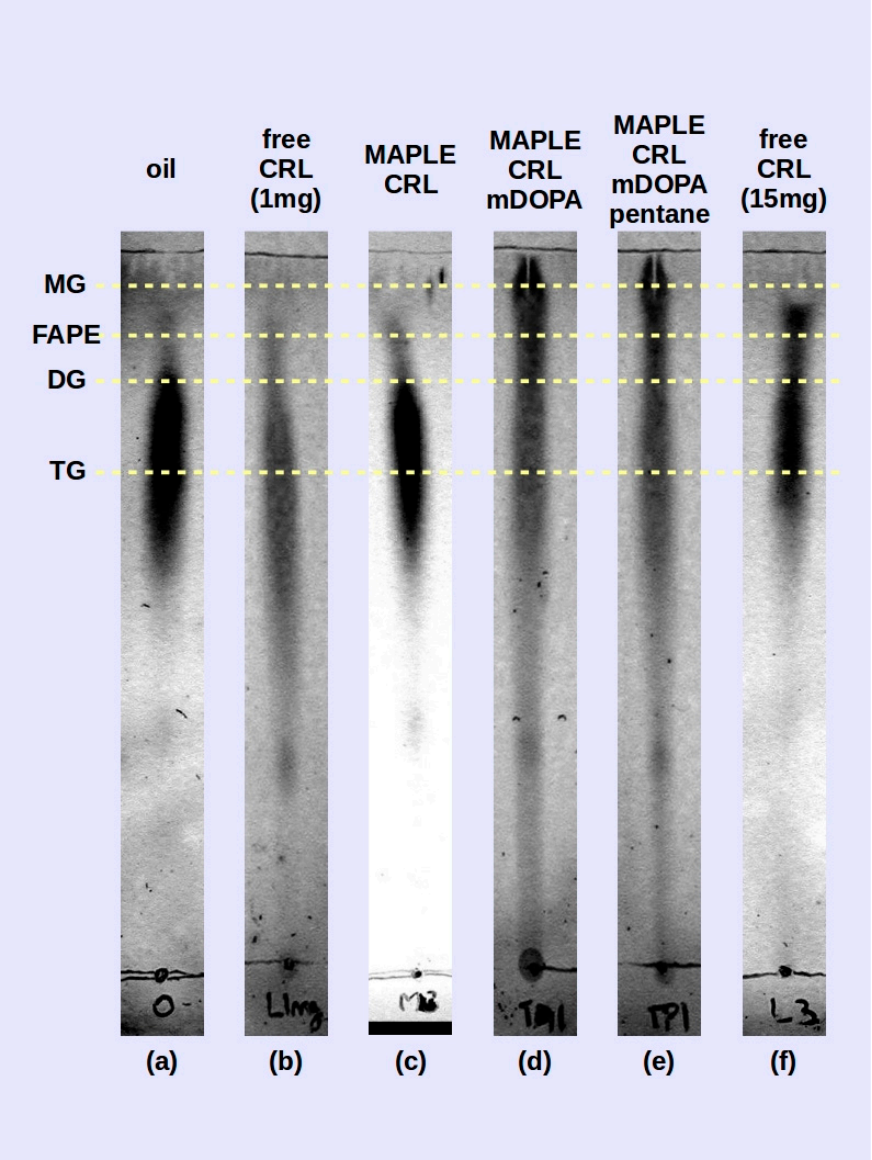


**Figure 5.** TLC of transesterification products obtained the MAPLE deposited lipase M-CRL1 (c), M-CRL2 (d) and M-CRL3 (e) as biocatalysts are compared to the chromatogram of the unreacted oil (a) and that obtained using 1mg (b) and 15 mg (f) of free-CRL as biocatalyst

On the RP-TLC plate the oil chromatogram shown in fig.5a appears elongated due to the variation in saturation and chain length of the component fatty acids [37]. For the reacted mixtures, the order of retention follows the polarity of the components: monoglycerides (MG) exhibit the least retention, followed by fatty acid propyl esters (FAPE), diglycerides (DG) and residual oil (TG, triglycerides) [37]. The RP-TLC results obtained using M-CRL1 as biocatalyst confirm the data obtained with GC-MS analysis, carried out in a previous study [10], allowing to identify peaks belonging to isopropyl esters of the most abundant fatty acid components of soybean oil, indicating that MAPLE deposited CRL preserved its functional role.

In the reacted mixture obtained using M-CRL2 (MAPLE deposited CRL with m-DOPA addition) and M-CRL3 (MAPLE deposited CRL with m-DOPA and pentane addition) lipase there is

Peer-reviewed version available at Molecules 2017, 22, 2153; doi:10.3390/molecules22122153



a higher quantity of MG and DG and a much lower quantity of FAPE with respect to the reaction mixture obtained with free-CRL. This occurrence appears unusual since CRL is a non specific lipase, and in this kind of biocatalysts the reaction intermediates MG and DG do not accumulate since they react faster than the TG [38]. Actually, comparison of TLC analysis performed on the reaction mixture obtained using 1 mg (fig.5b) and 15 mg (fig.5b) of free-CRL shows that despite the smaller quantity of FAPE obtained, reaction intermediates DG and MG are not produced. We hypothesize that the higher production of MG and DG is due to the conformational changes induced in the lipase during the MAPLE process and evidenced by the FTIR analysis. Nevertheless, the presence of KBr as immobilization support is also important, since the presence of a salt can lead to the formation of fatty acid salts, which in turn may lead to enzyme inhibition through conformational changes induced by the electrostatic interaction between the anionic headgroup and sites of opposite charge on the protein [38].

## 3. Materials and Methods

About 2 mL of the target solution were placed into the target holder and frozen by thermal contact with liquid nitrogen. The deposition chamber was evacuated and afterwards the Nd:YAG pulsed laser was switched on to start the deposition. The target holder was moved by a computer controlled mechanical system so that the laser beam scanned an area of about 1.5 $cm^2$ in order to prevent local overheating and drilling of the target. The MAPLE targets were prepared by dissolving the appropriate quantity of lipase in water (M-CRL1), then adding the required amount of m-DOPA aqueous solution (M-CLR2) and of pentane (M-CLR3) and finally refrigerating the mixture at liquid nitrogen temperature.

Lipase films were deposited on KBr pellets of 13 mm diameter in order to perform FTIR analysis. FTIR spectra were recorded, in the 4000-400 $cm^{-1}$ range, using a spectrometer equipped with a DTGS KBr (deuterated triglycine sulphate with potassium bromide windows) detector. A spectral resolution of 2 $cm^{-1}$ was chosen and each spectrum represents an average of 64 scans, corrected for the spectrum of the blank KBr pellet. For comparison, spectra were acquired also for lyophilized unprocessed lipase (free-CRL). 4.0 mg of lyophilized lipase were mixed with 196 mg of KBr and pressed into pellets. The salt was previously dried at 100 ° C for 24 h in order to eliminate the interference of water in the spectra. The curve fitting of the amide I band was performed with curve-fit procedure of GRAMS/32, after smoothing and baseline subtraction. All spectra were analyzed by the second derivative method to determine the number of peaks to use as input parameters of the fitting. Curves were fitted with Gaussian function choosing as initial full width at half height (FWHH) 12 $cm^{-1}$. Fitting was automatically performed by iterative adjustment of data until convergence.

Images of the deposited CRL films on KBr substrate were obtained by means of an Olympus microscope with 100X magnification, using a micrometric slide to quantify the size of the aggregates formed in the process.

The typical sample morphology was determined by atomic force microscopy (AFM) analysis of deposits obtained onto KBr substrates. The analysis was performed by means of a Nanoscope IIIa AFM (Veeco Instruments Inc., USA), operating in tapping mode (scan size and rate of 1 μm and 1 Hz, respectively), equipped with a silicon tip having nominal curvature radius of about 5 nm.

In order to assess the ability of the deposited lipase to perform their catalytic role, transesterification reaction were carried out between soybean oil and isopropyl alcohol at 25°C for 24h, using the surfactant span 80® to emulsify the reactants. The reaction products were qualitatively characterized by reverse phase thin layer chromatography (RP-TLC), using precoated glass plates RP-18 and acetonitrile-ethylacetate 2.5:1 as mobile phase. The chromatograms were detected by spraying sulphuric acid 4 N on the chromatographic plates and heating them at 150 °C.

## 4. Conclusions

Candida Rugosa Lipase (CRL) is deposited by MAPLE tailoring the target composition in order to minimize the conformational modification observed during the process. In particular, a phenomenon of unfolding/aggregation is evidenced. Experimental results evidence that unfolding/aggregation induced by MAPLE process can be minimized by tailoring the target matrix: the addition of the amino acid m-DOPA is able to prevent aggregation, while the addition of pentane to form a microemulsion is effective for preventing unfolding. All MAPLE deposited samples show catalytic ability, but reaction privileges MG and DG products differently with respect to free-CRL which can be due to the MAPLE induced conformational modification of the deposited lipases together with other effects (influence of the support). The addition of an apolar solvent to the MAPLE target attenuates the conformational alteration occurring during MAPLE process, which represents a feasible way to maintain unaltered the conformation of the enzyme during the MAPLE deposition.

**Author Contributions:** F. Bloisi and L. Vicari carried out MAPLE depositions. A. Aronne and A. Costantini performed FTIR and data analysis. G. Ausanio is responsible for AFM measurements and G. Perretta carried out TLC. V. Califano wrote the paper and contributed in all experimental measurements and data elaboration.

The authors declare no conflict of interest

## References

1. Knêzevíc, Z.D.; ˇSiler-Marinkovíc, S.S.; Mojovíc, L.V. Immobilized lipases as practical catalysts. APTEFF 2004, 35, 151–164. 10.2298/apt0435151k.
2. Sellinger, A.T;. Leveugle, E.; Gogick, K.; Peman, G.; Zhigilei, L.V.; Fitz-Gerald, J.M. Ejection of matrix-polymer clusters in matrix assisted laser evaporation: experimental observations. J. Phys.: Conf. Ser. 2007, 59, 314–317. 10.1088/1742-6596/59/1/027.
3. Esenaliev, R.O.; Karabutov, A.A.; Podymova, N.B.; Letokhov, V.S. Laser ablation of aqueous solutions with spatially homogeneous and heterogeneous absorption. Appl. Phys. B: Lasers Opt. 1994, 59, 73–81. 10.1007/BF01081730.Author 1, A.B.; Author 2, C. Title of Unpublished Work.
4. Shepard, K.B.; Priestley, R.D. MAPLE deposition of macromolecules. Macromol. Chem. Phys. 2013, 214, 862-870. 10.1002/macp.201200621.
5. Cristescu, R.; Mihaiescu, D.; Socol, G.; Stamatin, I.; Mihailescu, I.N.; Chrisey, D.B. Deposition of biopolymer thin films by matrix assisted pulsed laser evaporation. Appl. Phys. A: Mater. Sci. Process. 2004, 79, 1023–1026. 10.1007/s00339-004-2619-9.
6. Stamatin, L.; Cristescu, R.; Socol, G.; Moldovan, A.; Mihaiescu, D.; Stamatin, I.; Mihailescu, I.N.; Chrisey, D.B. Laser Deposition of fibrinogen blood proteins thin films by matrix assisted pulsed laser evaporation. Appl. Surf. Sci. 2005, 248, 422–427. 10.1016/j.apsusc.2005.03.060.
7. Ringeisen, B.R.; Callahan, J.; Wu, P.K.; Piqué, A.; Spargo, B.; McGill, R.A.; Bucaro, M.; Kim, H.; Bubb, D.M.; Chrisey, D.B. Novel laser-based deposition of active protein thin films. Langmuir 2001, 17, 3472-3479. 10.1021/la0016874.
8. Purice, A.; Schou, J.; Kingshott, P.; Pryds, N.; Dinescu, M. Characterization of lysozyme films produced by matrix assisted pulsed laser evaporation (MAPLE). Appl. Surf. Sci. 2007, 253, 6451-6455. 10.1016/j.apsusc.2007.01.066.
9. Domínguez de María, P.; Sánchez-Montero, J.M.; Sinisterra, J.V.; Alcántara, A.R. Understanding candida rugosa lipases: an overview. Biotechnol. Advances 2006, 24, 180-196. 10.1016/j.biotechadv.2005.09.003.
10. Aronne, A.; Ausanio, G.; Bloisi, F.; Calabria, R.; Califano, V.; Fanelli, E.; Massoli, P.; Vicari, L.R.M. Structural characterization of MAPLE deposited lipase biofilm. Appl. Surf. Sci. 2014, 320, 524–530. 10.1016/j.apsusc.2014.09.112.
11. Califano, V.; Bloisi, F.; Vicari, L.R.M.; Colombi, P.; Bontempi, E.; Depero, L.E. MAPLE deposition of biomaterial multilayers. Appl. Surf. Sci. 2008, 254, 7143-7148. 10.1016/j.apsusc.2008.05.295.
12. Tian, F.; Middaugh, C.R.; Offerdahl, T.; Munson, E.; Sane, S.; Rytting, J.H. Spectroscopic evaluation of the stabilization of humanized monoclonal antibodies in amino acid formulations. Int. J. Pharm. 2007, 335, 20–31. 10.1016/j.ijpharm.2006.10.037.
13. Foresti, M.L.; Ferreira, M.L. Frequent analytical/experimental problems in lipase-mediated synthesis in solvent-free systems and how to avoid them. Anal. Bioanal. Chem. 2005, 38, 1408-1425. 10.1007/s00216-005-3087-6.
14. Greer, J.A. Design challenges for matrix assisted pulsed laser evaporation and infrared resonant laser evaporation equipment. Appl. Phys. A: Mater. Sci. Process. 2011, 105, 661–671. 10.1007/s00339-011-6611-x.
15. Stenberg, B.; Viscarra Rossel, R.A.; Mouazen, A.M.; Wetterlind, J. Advances in Agronomy. D.L. Sparks, Academic Press 2010 pp 163-215.
16. Maçzyński, A.; Wiśniewska-Gocłowska, B.; Góral, M. Recommended liquid–liquid equilibrium data. Part 1. Binary alkane–water systems. J. Phys. Chem. Ref. Data 2004, 33, 549-577. 10.1063/1.1643922.
17. Flanagan, J.; Singh, H.; Microemulsions: a potential delivery system for bioactives in food. Crit. Rev. Food Sci. Nutr. 2006, 46, 211-237. 10.1080/10408690590956710.
18. Paul, B.K.; Moulik, S.P. Microemulsions: an overview. J. Dispersion Sci. Technol. 1997, 18, 301-367. 10.1080/01932699708943740.
19. Ghosh, S.; Coupland, J.N.; Factors affecting the freeze–thaw stability of emulsions. Food Hydrocolloids 2008, 22, 105–111. 10.1016/j.foodhyd.2007.04.013.

20. Cramp, G.L.; Docking, A.M.; Ghosh, S.; Coupland, J.N. On the stability of oil-in-water emulsions to freezing. Food Hydrocolloids 2004, 18, 899-905. 10.1016/j.foodhyd.2003.10.007.
21. Arrondo, J.L.R.; Muga, A.; Castresana, J.; Goni, F.M. Quantitative studies of the structure of proteins in solution by Fourier-transform infrared spectroscopy. Prog. Biophys. Mol. Biol. 1993, 59, 23–56. 10.1016/0079-6107(93)90006-6.
22. Natalello, A., Ami, D.; Brocca, S.; Lotti, M.; Doglia, S.M. Secondary structure, conformational stability and glycosylation of a recombinant Candida Rugosa lipase studied by Fourier-transform infrared spectroscopy. Biochem. J. 2005, 385, 511–517. 10.1042/BJ20041296.
23. Ranaldi, S.; Belle, V.; Rodriguez, J.; Guigliarelli, B.; Sturgis, J.; Carriere, F.; Fournel, A. Lid opening and unfolding in human pancreatic lipase at low pH revealed by site-directed spin labeling EPR and FTIR spectroscopy. Biochemistry 2009, 48, 630–638. 10.1021/bi801250s.
24. Zhou, Z.; Inayat, A.; Schwieger, W.; Hartmann, M. Improved activity and stability of lipase immobilized in cage-like large pore mesoporous organosilicas, Microporous Mesoporous Mater. 2012, 154, 133–141. 10.1016/j.micromeso.2012.01.003.
25. Noinville, S.; Revault, M.; Baron, M.; Tiss, A.; Yapoudjian, S.; Ivanova, M.; Verger, R. Conformational changes and orientation of Humicola Lanuginosa lipase on a solid hydrophobic surface: an in situ interface Fourier transform infrared-attenuated total reflection study. Biophys. J. 2002, 82, 2709–2719. 10.1016/S0006-3495(02)75612-9.
26. Narayanan, P. Essential of Biophysics, New Age International Ed, New Delhi, 2000, p 219.
27. van Stokkum, I.H.M.; Linsdell, H.; Hadden, J.M.; Hais, P.I.; Chapman, D.; Bloemendal, M. Temperature-induced changes in protein structures studied by Fourier transform infrared spectroscopy and global analysis. Biochemistry 1995, 34, 10508-10518. 10.1021/bi00033a024.
28. Kong, J.; Yu, S.; Fourier transform infrared spectroscopic analysis of protein secondary structures. Acta Biochim. Biophys. Sin. 2007, 39, 549–559. 10.1111/j.1745-7270.2007.00320.x.
29. Chronopoulou, L.; Kamel, G.; Sparago, C.; Bordi, F.; Lupi, S.; Diociaiuti, M.; Palocci, C. Structure-activity relationships of Candida rugosa lipase immobilized on polylactic acid nanoparticles. Soft Matter 2011,7, 2653-2662. 10.1039/C0SM00712A.
30. Grochulski, P.; Li, Y.; Schrag, J.D.; Cygler, M. Two conformational states of Candida rugosa lipase, Protein Sci. 1994, 3, 82–91. 10.1002/pro.5560030111.
31. Bloisi, F.; Califano, V.; Perretta, G.; Nasti, L.; Aronne, A.; Di Girolamo, R.; Auriemma, F.; De Rosa, C.; Vicari, L.R. Lipase immobilization for catalytic applications obtained using fumed silica deposited with MAPLE technique. Appl. Surf. Sci. 2015, 374, 346-352. 10.1016/j.apsusc.2015.12.131.
32. Sucharda-Sobczyk, A.; Siemion, I.Z.; Konopinska, D. Infrared spectroscopic investigations of tuftsin and its analogs. Eur. J. Biochem. 1979, 96, 131-139. 10.1111/j.1432-1033.1979.tb13022.x.
33. Gutiérrez-Llorente, A.; Horowitz, G.; Pérez-Casero, R.; Perriére, J.; Fave, J.L.; Yassar, A.; Sant, C. Growth of polyalkylthiophene films by matrix assisted pulsed laser evaporation. Org. Electron. 2004, 5, 29-34. 10.1016/j.orgel.2003.11.003.
34. Gupta, R.K.; Ghosh, K.; Kahol, P.K.; Yoon, J.; Guha, S. Pulsed laser thin film growth of di-octyl substituted polyfluorene and its co-polymers. Appl. Surf. Sci. 2008, 254, 7069-7073. 10.1016/j.apsusc.2008.05.198.
35. Bubb, D.M.; Corgan, J.; Yi, S.Y.; Khan, M.; Hughes, L.; Gurudas, U.; Papantonakis, M.; McGill, R.A. An experimental investigation of inhomogeneities in resonant infrared matrix-assisted pulsed-laser deposited thin polymer films. Appl. Phys. A: Mater. Sci. Process. 2010, 100, 523-531. 10.1007/s00339-010-5854-2.
36. Zhigilei, L.V.; Volkov, A.N.; Leveugle, E.; Tabetah, M. The effect of the target structure and composition on the ejection and transport of polymer molecules and carbon nanotubes in matrix-assisted pulsed laser evaporation. Appl. Phys. A: Mater. Sci. Process. 2011, 10, 529–546. 10.1007/s00339-011-6595-6.
37. Wall, P.E. III\Triglycerides\Thin-Layer (Planar) Chromatography in I.D. Wilson, M. Cooke, C.F. Poole (Eds.), Encyclopedia of separation science, Academic Press, London, 2000, pp. 4412-4420.
38. Illanes, A. Enzyme Biocatalysis: Principles and Applications, Springer Science & Business Media, 2008, p.299.
39. Reis, P.; Miller, R.; Leser, M.; Watzke, H. Lipase-catalyzed reactions at interfaces of two-phase systems and microemulsions, Appl. Biochem. Biotechnol. 2009, 158, 706–721. 10.1007/s12010-008-8354-5.